Global patterns in leaf ^{13}C discrimination and implications for studies of past and future climate

Aaron F. Diefendorf[a1,2], Kevin E. Mueller[b1], Scott. L. Wing[c], Paul L. Koch[d], and Katherine H. Freeman[a]

[a]Department of Geosciences, Pennsylvania State University, University Park, PA 16802; [b]Intercollege Degree Program in Ecology, Pennsylvania State University, University Park, PA 16802; [c]Department of Paleobiology, P.O. Box 37012, Smithsonian Institution, National Museum of Natural History Washington, DC 20013; and [d]Department of Earth and Planetary Sciences, University of California, Santa Cruz, CA 95064

Edited by John M. Hayes, Woods Hole Oceanographic Institution, Berkeley, CA, and approved February 3, 2010 (received for review September 14, 2009)

Fractionation of carbon isotopes by plants during CO_2 uptake and fixation (Δ_{leaf}) varies with environmental conditions, but quantitative patterns of Δ_{leaf} across environmental gradients at the global scale are lacking. This impedes interpretation of variability in ancient terrestrial organic matter, which encodes climatic and ecological signals. To address this problem, we converted 3,310 published leaf $\delta^{13}C$ values into mean Δ_{leaf} values for 334 woody plant species at 105 locations (yielding 570 species-site combinations) representing a wide range of environmental conditions. Our analyses reveal a strong positive correlation between Δ_{leaf} and mean annual precipitation (MAP; $R^2 = 0.55$), mirroring global trends in gross primary production and indicating stomatal constraints on leaf gas-exchange, mediated by water supply, are the dominant control of Δ_{leaf} at large spatial scales. Independent of MAP, we show a lesser, negative effect of altitude on Δ_{leaf} and minor effects of temperature and latitude. After accounting for these factors, mean Δ_{leaf} of evergreen gymnosperms is lower (by 1–2.7‰) than for other woody plant functional types (PFT), likely due to greater leaf-level water-use efficiency. Together, environmental and PFT effects contribute to differences in mean Δ_{leaf} of up to 6‰ between biomes. Coupling geologic indicators of ancient precipitation and PFT (or biome) with modern Δ_{leaf} patterns has potential to yield more robust reconstructions of atmospheric $\delta^{13}C$ values, leading to better constraints on past greenhouse-gas perturbations. Accordingly, we estimate a 4.6‰ decline in the $\delta^{13}C$ of atmospheric CO_2 at the onset of the Paleocene-Eocene Thermal Maximum, an abrupt global warming event ~55.8 Ma.

biogeochemistry | ecophysiology | fractionation | PETM

Human perturbation of the global carbon (C) cycle is potentially far greater in rate and magnitude than variations in the recent past, pushing predictions of future climate beyond the calibration range of models based on modern and near-modern observations. Robust predictions of future impacts of rising CO_2 require not only extrapolation of ecological patterns along modern environmental gradients but also insights gained from changing ecological patterns at times of high CO_2 and hot climate in the geologic past (1 and 2). Global patterns of variation in leaf carbon isotope ($\delta^{13}C_{leaf}$) values potentially record climate-driven changes in modern plant physiology and biogeochemistry. An understanding of factors controlling plant fractionation (Δ_{leaf}) at the global scale will improve interpretations of past changes in climate and ecology recorded in ancient terrestrial sedimentary organic carbon (2). Patterns in $\delta^{13}C_{leaf}$ of living plants at the global scale, however, are unresolved in spite of abundant published data at smaller spatial scales.

In living plants, $\delta^{13}C_{leaf}$ values reflect the balance of photosynthesis and stomatal conductance and their coupled response to the environment (3). Edaphic factors (e.g., water availability, altitude, temperature) and plant attributes (e.g. phylogeny and leaf traits) can influence $\delta^{13}C_{leaf}$ values (4–6). The relative importance of these factors at the global scale is not known, nor is it clear how they might drive the variations in ancient $\delta^{13}C_{leaf}$ values recorded in either terrestrial organic carbon ($\delta^{13}C_{TOC}$) or $\delta^{13}C$ values of plant biomarkers.

During extreme climate events in the past, changes in the isotope ratio of atmospheric CO_2 ($\delta^{13}C_{atm}$) reflect perturbations in atmospheric C fluxes, therefore accurate estimates of $\delta^{13}C_{atm}$ are central to estimating past climate sensitivity to changes in pCO_2 (7). Values of $\delta^{13}C_{TOC}$ from sedimentary rocks are widely used to estimate $\delta^{13}C_{leaf}$ of ancient plants and infer changes in $\delta^{13}C_{atm}$ (8). However, the offset between $\delta^{13}C_{atm}$ and $\delta^{13}C_{leaf}$ (i.e., Δ_{leaf}) varies with climate and plant characteristics and such variations must be accounted for when estimating atmospheric C isotope excursions (CIE) from ancient plant-derived C. For example, during the Paleocene-Eocene Thermal Maximum (PETM), a period of rapid global warming 55.8 million years ago (9), the CIEs in terrestrial organic carbon (TOC) and atmospheric CO_2 likely differ because of changes in Δ_{leaf} that accompanied plant community shifts, warming (~5 °C), decreasing precipitation and increases in atmospheric CO_2 (2).

In this study, we provide predictive relationships for Δ_{leaf} variability of woody C_3 plants at the global scale from analysis of published $\delta^{13}C_{leaf}$ values, plant functional types, biome, climate, and geography. We use these relationships to show how environmental and ecologic change during the PETM influenced plant fractionation and therefore the CIE recorded by fossil leaf waxes.

Results and Discussion

Leaf Carbon Isotope Fractionation. We used Δ_{leaf} in our analyses as it controls for variation in $\delta^{13}C_{atm}$ (10). Δ_{leaf} in C_3 plants is a function of the fractionation associated with CO_2 diffusion (4.4%) and photosynthetic fractionation by Rubisco (27%). For C_3 plants, the concentration of CO_2 in the substomatal cavities of leaves (c_i) is directly proportional to Δ_{leaf} when the atmospheric CO_2 concentration (c_a) is held constant (10) (but see ref. 11). In turn, c_i depends on the flux of CO_2 into the leaf, which is largely regulated by stomatal conductance (g_s) and the flux of CO_2 removed from the leaf for C fixation by assimilation (A) (10). Values of Δ_{leaf} generally decrease with reductions in water availability, reflecting a down-regulation of g_s and increased water-use efficiency (WUE) (10, 12). Thus, Δ_{leaf} is a time-integrated measure of WUE, although leaf temperature (T), mesophyll conductance and differences in c_a are potential confounding factors (11 and 13). Confounding effects are reduced, however, because mesophyll conductance is correlated with A (and with g_s) (11 and 14) and trees appear to maintain leaf

Author contributions: A.F.D., K.E.M., and K.H.F. designed research; A.F.D., K.E.M., S.L.W., and P.L.K. performed research; A.F.D. and K.E.M. analyzed data; and A.F.D., K.E.M., S.L.W., P.L.K., and K.H.F. wrote the paper.

The authors declare no conflict of interest.

This article is a PNAS Direct Submission.

[1]A.F.D. and K.E.M. contributed equally to this work.

[2]To whom correspondence should be addressed. E-mail: aaron.diefendorf@gmail.com.

This article contains supporting information online at www.pnas.org/cgi/content/full/0910513107/DCSupplemental.

www.pnas.org/cgi/doi/10.1073/pnas.0910513107

T within a narrow range (21.4 ± 2.2 °C) across a wide range of ambient T (15). A and g_s also vary with plant phylogeny, growth form and leaf traits, thus Δ_{leaf} and its response to the environment may differ for plant functional types (PFTs) defined by these attributes (4).

Data. Our dataset, provided in Dataset S1, includes 334 species from 75 woody plant families (including trees and shrubs) present at 105 geographic sites distributed across 5 continents (representing 3,310 $\delta^{13}C_{leaf}$ measurements of individual plants). The result is 570 unique species-site combinations represented by a mean Δ_{leaf} value calculated from multiple individuals of each species at a site. These sites represent eight biomes with mean annual temperature ranging from −10° to 28 °C and mean annual precipitation (MAP) from 147 to 3,700 mm per year, capturing the broad range in which higher plants occur (*SI Appendix*).

Precipitation. MAP is positively correlated to global Δ_{leaf} values ($p < 0.0001$, $R^2 = 0.55$; Fig. 1) and is the strongest predictor of Δ_{leaf} among the environmental parameters in our dataset. To our knowledge this study represents the largest spatial scale at which this correlation has been documented, though it has been seen in some, but not all, regional studies and with considerably lower explanatory power (16–20). The strong correlation of MAP with Δ_{leaf} suggests that as water availability increases, stomatal limitations on c_i and A relax and WUE declines (i.e., g_s increases relative to A), leading to greater absolute C fixation (3 and 10). These apparent stomatal limitations on leaf-level A likely scale up to the ecosystem level and help explain global variation in gross and net primary production, which also varies with MAP (21).

The relationship between MAP and Δ_{leaf} is consistently strong within the continents of North America (NA) and Asia (*SI Appendix*), but not Europe (EU; $R^2 = 0.025$, $p = 0.125$). Extensive analysis of European data does not reveal any single environmental variable (or simple combination of variables) that accounts for more than 20% of the variation in Δ_{leaf} across all plant types. The lack of strong MAP effects on Δ_{leaf} in EU (see also ref. 16) and elsewhere (17–19) may arise from heterogeneity in growing season water availability that is not captured by MAP, due to differences in the seasonality of rainfall across sites (i.e. EU includes areas with wet winters in the south and wet summers in the north) or the presence of sites where soil water does not come from local precipitation. Better measures of water availability during growth may yield different results. For example, in our NA dataset, summer precipitation (June to August) is a better estimate of water availability than MAP for deciduous angiosperms and is more strongly correlated with Δ_{leaf} ($R^2 = 0.83$ and 0.57 respectively, $p < 0.0001$, $n = 36$ species-site combinations, excluding tropical sites and one California site with a wet winter).

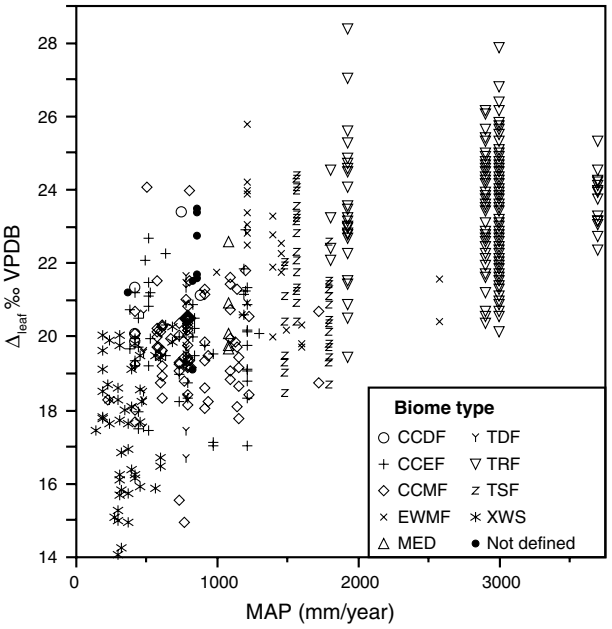

Fig. 1. Effect of mean annual precipitation (MAP) on Δ_{leaf} ($n = 506$). MAP accounts for 55% ($p < 0.0001$) of the variability in Δ_{leaf} in a linear regression model. Points are coded by biome: tropical rain forest (TRF), evergreen warm mixed forest (EWMF), tropical seasonal forest (TSF), cool-cold deciduous forest (CCDF), cool-cold evergreen forest (CCEF), cool-cold mixed forest (CCMF), tropical deciduous forest (TDF), xeric woodland scrubland (XWS). In a regression model using site-means (Δ_{leaf} averaged by geographic location), MAP accounts for 52% ($p < 0.0001$) of the variability in Δ_{leaf} (*SI Appendix*).

Altitude and Other Factors. We assessed the influence of other factors on Δ_{leaf} using bivariate partial regression models that account for the covariance of MAP with other predictors (*SI Appendix*) and its correlation with Δ_{leaf}. This approach is justified by our observation that MAP emerges as the strongest single predictor of Δ_{leaf} and because the influence of MAP on Δ_{leaf} is supported by theory and other observations. The partial regression model with altitude as a secondary predictor is the only model with notable explanatory power ($R^2 = 0.13$, $p < 0.0001$) indicating that altitude has a weak, negative influence on Δ_{leaf} that is statistically independent of its covariance with MAP. The combination of MAP and altitude explains 61% of the global variability in Δ_{leaf} in a multiple regression model ($p < 0.0001$), and regression models for data-rich continents show similar results (*SI Appendix*). Elevation effects on Δ_{leaf} have been observed previously (3 and 20), although altitude is rarely evaluated independently of MAP. The responsible mechanisms remain uncertain (3) and could be related to T, vapor pressure, oxygen partial pressure, irradiance, or other factors.

MAP and altitude effects on Δ_{leaf} are evident when regressions are performed on data grouped by PFT (*SI Appendix*), indicating that their influence is independent of community changes along elevation or precipitation gradients. The effects of MAP and altitude are still apparent when regressions are performed separately for well represented genera in our database (*SI Appendix*). Phylogenetic variation is reduced within genera, making it unlikely that the global correlations of Δ_{leaf} with MAP (Fig. 1) and altitude are driven exclusively by differences in the taxonomic composition of floras in different regions. Rather, we suggest Δ_{leaf} is evolutionarily and physiologically plastic in response to changes in water availability.

Unexpectedly, other factors (e.g. T, latitude, evapotranspiration) were not significantly related to Δ_{leaf} after controlling for MAP and altitude in regression models of the entire dataset. Negligible effects of these factors could indicate that A and g_s covary more tightly with T and other factors than with changes in MAP and altitude. Covariance of T with MAP, altitude, or PFT distribution may also mask its influence (*SI Appendix*, see below).

Plant Functional Types. Despite the considerable variance in Δ_{leaf} explained by MAP and altitude, much remains unexplained, as evident by the ~8% range in Δ_{leaf} at any given MAP value (Fig 1; Dataset S1). Microclimate, ecosystem structure, and differences in plant traits among the species and PFTs must explain some of this variability. Several studies have reported localized differences in Δ_{leaf} among woody PFTs and similar results have been observed in metaanalyses of wood $\delta^{13}C$ (6). Yet previous metaanalyses of Δ_{leaf} of C_3 plants have not found evidence of a PFT effect (22), with the exception that grasses differ from woody plants (4). This likely reflects inadequate control for environmental influences on Δ_{leaf} that are independent of PFT. On the other

hand, accounting for the uneven distribution of PFTs along environmental gradients may reveal additional environmental controls on Δ_{leaf}. When regression models are analyzed separately for each PFT, small latitude and T effects on Δ_{leaf} are evident for deciduous angiosperms (DA) and evergreen gymnosperms (EG), the PFTs that span the greatest range in latitude and T (*SI Appendix*). For DAs and EGs, increases in latitude or decreases in T result in slightly higher Δ_{leaf} than predictions based on MAP and altitude alone, indicating limitations on carbon assimilation due to low T or irradiance.

We used a multiple regression model with MAP and altitude as predictors to capture the dominant environmental influences on Δ_{leaf}, and explored whether PFTs explain any residual variation in Δ_{leaf}. This approach reveals significant differences in Δ_{leaf} among PFTs (*SI Appendix*), with EGs between 1.0% and 1.5% lower than the others. More strict control of confounding environmental influences on Δ_{leaf} is achieved by limiting PFT comparisons to plants at the same geographic site (Fig. 2; *SI Appendix*). With this constraint, DAs and evergreen angiosperms (EA) have higher Δ_{leaf} than EGs, by 2.7% and 2.2% respectively. PFT effects on Δ_{leaf} are not solely related to phylogeny or leaf habit. These differences may be related to genetic or phenotypic differences in A and g_s mediated by leaf morphology, hydraulic architecture, rooting depth, leaf T, and/or mesophyll conductance (3, 10, 11, 13). These traits also vary among species *within* the same PFT; future studies should examine this variation.

Deciduous and evergreen species have contrasting nutrient use and retention strategies (23) that may underlie their dominance in different ecosystems. Our results support the notion that WUE differences are also an important component of plant strategies related to resource availability and likely help explain PFT dominance patterns. Lower Δ_{leaf} implies greater WUE of EGs relative to other woody plants, conferring a potential advantage where water is limiting and a limitation on A when water availability is high (24).

Biome Patterns. Mean Δ_{leaf} values calculated by biome type (Fig. 3; *SI Appendix*) differed significantly, with greatest fractionation in tropical rain forests (mean Δ_{leaf} = 23.4%) and lowest in xeric woodland/scrublands (mean Δ_{leaf} = 17.3%), which compare well with biome level Δ_{leaf} patterns predicted by Kaplan et al. (5). We

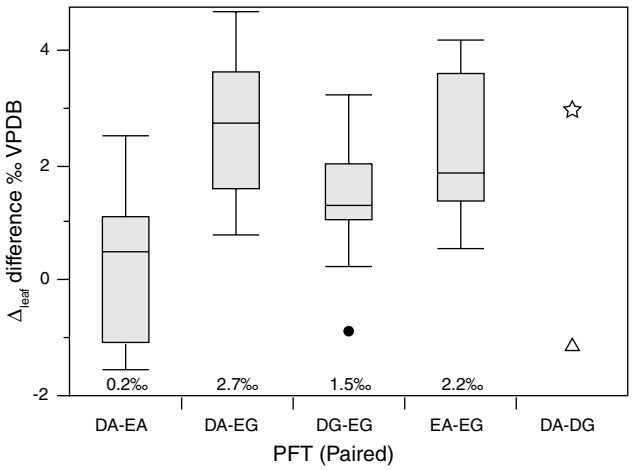

Fig. 2. Differences in Δ_{leaf} between cooccurring plant functional types (PFTs). For each geographic site, mean Δ_{leaf} values of each species were averaged to produce a mean Δ_{leaf} for each PFT. *Box* and *whisker* plots show the *median*, *upper* and *lower* quartiles, and *maximum* and *minimum* values, with outlier values shown as *black dots*. Number of sites per PFT comparison are as follows (deciduous angiosperm, DA; deciduous gymnosperm, DG; evergreen angiosperm, EA; evergreen gymnosperm, DG): DA – EA = 16, DA – EG = 17, DG – EG = 21, EA – EG = 12. DA-DG comparison is shown to highlight differences between *Larix* (*triangle*) and *Taxodium* (*star*).

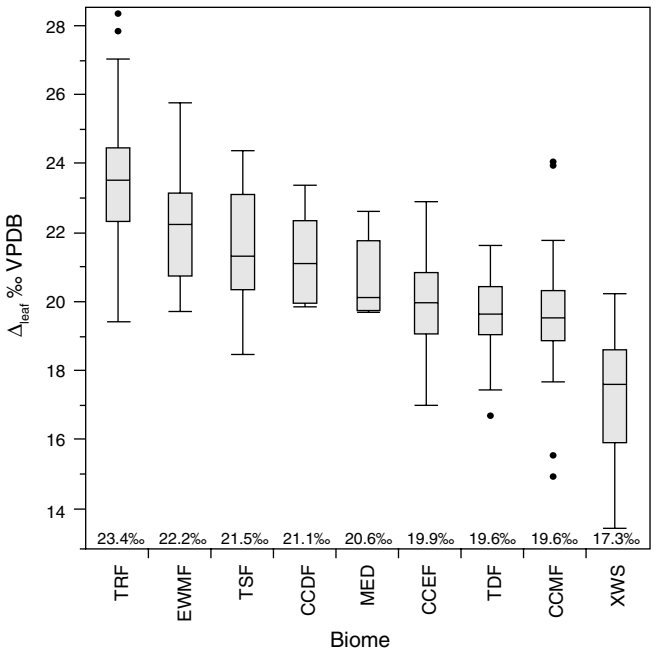

Fig. 3. *Box* and *whisker* plots of Δ_{leaf} values by biome. Biome accounts for 66% ($p < 0.0001$) of the variability in Δ_{leaf} in an ANOVA model. Number of samples per biome are as follows (see Fig. 1 caption for abbreviations): TRF = 206; EWMF = 29; TSF = 47; CCDF = 5; MED = 5; CCEF = 53; CCMF = 78; TDF = 26; XWS = 59. Statistical tests of means are shown in *SI Appendix*.

observe a similar pattern when mean Δ_{leaf} for each biome is calculated separately for angiosperms and gymnosperms (*SI Appendix*). Biome type alone explains more Δ_{leaf} variation than MAP (R^2 of 66% and 55%, respectively, *SI Appendix*), because it captures other factors related to Δ_{leaf}, including the spatial distribution of PFTs. PFT influences at the biome scale are readily apparent; cool-cold deciduous forests have higher Δ_{leaf} values (by 1.2%) than cool-cold evergreen forests (Fig. 3; see also Kaplan et al. (5)). The DA-EG differences in Δ_{leaf} (1.0% to 2.7%) calculated for each biome are consistent with results based on residuals of multiple regression (1.0–1.5%; *SI Appendix*) and the paired-site comparison (2.7%; Fig. 2).

Implications for Models. Kaplan et al. (5) recently extended a coupled vegetation-biogeochemical model (BIOME4) to predict Δ_{leaf} at the biome and PFT scale. Our database for C_3 woody plants provides a means for full evaluation of BIOME4's ability to reproduce global patterns in Δ_{leaf}. Since Δ_{leaf} records the time-integrated balance of A and g_s, global patterns in Δ_{leaf} can be used to assess the ability of physiological models to predict the balance between leaf C and H_2O fluxes. Further, incorporating Δ_{leaf} into coupled vegetation-biogeochemistry models have potential to enable predictive mapping of spatial variability in $\delta^{13}C_{leaf}$ and $\delta^{13}C_{TOC}$, which could improve studies of the effect of climate on modern and ancient organic matter.

Geologic Implications. The importance of water in regulating Δ_{leaf} values is often invoked in environmental and atmospheric reconstructions from $\delta^{13}C_{TOC}$ (1). More recently, the role of PFTs in controlling $\delta^{13}C_{TOC}$ has been identified (2 and 25). Our results show that variation in PFT and MAP independently result in differences in Δ_{leaf} of up to several ‰ (Fig. 1 and 2), and that biome may be a powerful integrator of PFT, rainfall, and other effects on Δ_{leaf} and $\delta^{13}C_{TOC}$ (Fig. 3). These quantitative relationships can be used to understand temporal and spatial variations in $\delta^{13}C_{TOC}$ provided that MAP and PFT (or biome) can be estimated in the geologic past.

There are uniformitarian assumptions in using Δ_{leaf} patterns among extant plants to interpret the vegetation of the geological past, however two factors encourage us to proceed. First, the morphological and physiological responses of C_3 plants to water stress are constrained by their fundamental anatomy and biochemistry (26), making it likely that the relationship of water availability and Δ_{leaf} has been similar in direction and magnitude over geological time. MAP and altitude effects on Δ_{leaf} are apparent within as well as among genera, implying that independent lineages respond similarly and quickly. Second, a recent study by Crisp et al. (27) shows that plant lineages rarely shift biomes during evolution, suggesting niche conservatism and supporting the careful use of biome type to constrain Δ_{leaf} values. Nonetheless, applying modern correlations of Δ_{leaf} with environment to the distant geological past may be problematic because of differences in major plant groups prior to the origin of angiosperms in the Cretaceous.

Pollen and leaf fossils document spatial and temporal changes in PFT as well as *T* and precipitation (9 and 28). Plant biomarkers (chemical fossils), such as *n*-alkanes (from leaf waxes) or terpenoids (defense compounds) are also preserved geologically (9) and have fewer diagenetic or source effects on their isotopic composition than $\delta^{13}C_{TOC}$ (29). Plant waxes in ancient sediments reflect productivity-weighted inputs from all PFTs contributing to that deposit. The resulting mixed molecular signal can be used to estimate a $\delta^{13}C_{leaf}$ value that integrates plant biomass within the catchment. In contrast, terpenoids provide PFT specificity because tricyclic diterpenoids are unique to woody gymnosperms and pentacyclic triterpenoids are unique to woody angiosperms. Therefore, ratios of these terpenoids, after accounting for production and preservational biases, may provide estimates of PFT (30). Also, terpenoid $\delta^{13}C$ values can be used to calculate PFT-specific Δ_{leaf} values (25).

Heterogeneity in rainfall and PFT dominance across ancient landscapes presumably created spatial patterns in Δ_{leaf} just as they do now, even at small spatial scales. To understand differences in $\delta^{13}C_{TOC}$, $\delta^{13}C_{biomarkers}$ and the magnitude of CIEs recorded in different regions at the same time, and improve chemostratigraphic correlations using $\delta^{13}C_{TOC}$, we should account for biome (5), precipitation (9), and PFT (2 and 25) effects on Δ_{leaf} values using relationships like those reported above.

An important goal in studies that document temporal variation in $\delta^{13}C_{atm}$ is to reconstruct the sources and fluxes of C to the ancient atmosphere (7). $\delta^{13}C_{leaf}$ and $\delta^{13}C_{TOC}$ have been used to directly represent $\delta^{13}C_{atm}$ (4 and 31), but this approach is fraught with uncertainty (32). It has been suggested that using a simple numerical offset to convert $\delta^{13}C_{TOC}$ to $\delta^{13}C_{atm}$ under nonlimiting water conditions is sufficient to control for environmental impacts (4). To the contrary, we argue that secular changes in PFT and climate must also result in significant—but often unaccounted—effects on Δ_{leaf}. Previous studies averaged multiple $\delta^{13}C_{TOC}$ values to remove variation caused by environmental factors (4, 31, 32), ignoring insights about paleoecology and climate that might be inferred from $\delta^{13}C_{TOC}$ variations.

We use an example from the PETM to illustrate how our study of modern Δ_{leaf} can improve interpretation of ancient $\delta^{13}C_{biomarkers}$ and $\delta^{13}C_{atm}$ (Fig. 4; see *SI Appendix*). Smith et al. (2) documented a shift from a mixed angiosperm-conifer flora (~25% angiosperm) in the late Paleocene to an angiosperm flora (~100%) at the onset of the CIE, and inferred that the 5‰ decrease in $\delta^{13}C_{leaf}$ (estimated from *n*-alkanes) reflected both a decrease in $\delta^{13}C_{atm}$ (3–4‰) and an increase in Δ_{leaf} caused by a shift from conifers to angiosperms (1–2‰, (2, 9)). Although the dominant late Paleocene conifers in the Bighorn Basin (*Metasequoia* and *Glyptostrobus* (9 and 33)) were deciduous, they probably had low Δ_{leaf}, as do their extant relatives (34 and 35) (Fig. 2). Yet the PETM in Wyoming is also marked by a change from wetter conditions (MAP ~ 1,380 mm/yr) in the late Paleocene (28) to drier conditions (MAP ~ 800 mm/yr) at the onset of the event (9), which should have decreased Δ_{leaf}. When both PFT and MAP effects on Δ_{leaf} are taken into account (Fig. 4; see *SI Appendix*), the decrease in Δ_{leaf} from declining MAP is countered by the increase in angiosperms, resulting in a net Δ_{leaf} increase of 0.2‰ and an estimated negative CIE in $\delta^{13}C_{atm}$ of 4.6‰. This estimate of the atmospheric CIE is larger than that calculated by Smith et al. (2), who argued the CIE in $\delta^{13}C_{alkanes}$ was higher than the atmospheric CIE because of the loss of conifers, and that marine sediments recorded the true CIE. Our Δ_{leaf} correction for both PFT and MAP effects on $\delta^{13}C_{alkanes}$ suggests the relatively large CIE recorded in the Bighorn Basin and other terrestrial sites (36) may equal the atmospheric CIE. This larger CIE falls within the range recently reported from well-preserved shallow marine carbonate records (−3.5‰ to −5.0‰) and supports the notion that −3.5‰ is too small (37). A larger atmospheric CIE implies the carbon released at the onset of the PETM was more depleted or greater in mass than presently thought. Adjusting other terrestrial CIE records for biome, MAP, and PFT effects should further refine and reconcile estimates of the magnitude of the CIE.

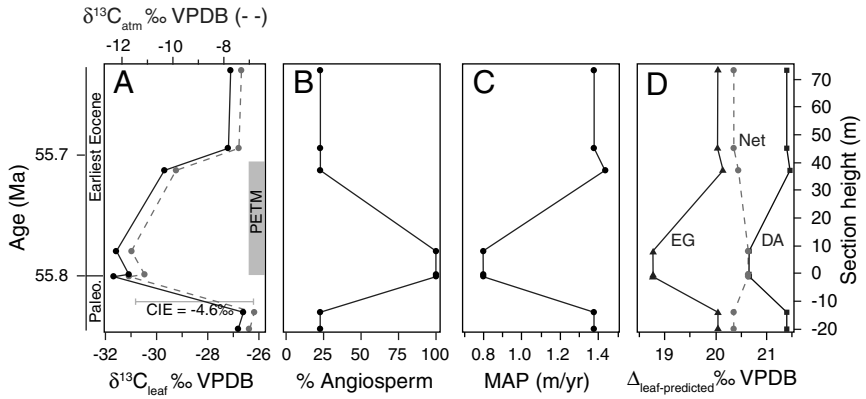

Fig. 4. Conceptual diagram of $\delta^{13}C_{atm}$ reconstruction for latest Paleocene to earliest Eocene sediments in the Bighorn Basin (WY). The figures are constructed as follows: (*A*) $\delta^{13}C_{leaf}$ values as inferred from $\delta^{13}C$ values of *n*-C_{31} alkanes (2), (*B*) percent of fossil leaves that are angiosperms, (*C*) mean annual precipitation (MAP) derived from fossil leaf metrics (9, 28), and (*D*) modeled net Δ_{leaf} from our Δ_{leaf}-MAP expressions for evergreen gymnosperm (EG; *triangles*) and deciduous angiosperm (DA; *squares*) PFTs (see *SI Appendix*). Each model was scaled by % angiosperm to derive a net Δ_{leaf} (*dashed line*). $\delta^{13}C_{atm}$ is denoted with a *dashed line* on *A* and is derived from the net Δ_{leaf} and $\delta^{13}C_{leaf}$ values. The negative CIE in $\delta^{13}C_{atm}$ at the base of the Paleocene-Eocene Thermal Maximum (PETM) is 4.6‰ (difference between latest Paleocene value and average of initial PETM values). See *SI Appendix* for discussion of calculations and suggested use of these models.

Relationships based on modern plants may not fully quantify the response of Δ_{leaf} to greenhouse climate conditions (high T and pCO_2) such as those of the PETM (12, 13, 38). Given the multiple functions of stomata (water loss prevention, CO_2 provision for A, evaporative cooling), it is unlikely that plants could simultaneously maintain homeostasis with respect to leaf T (15) and c_i or Δ_{leaf} (12) during periods of rapid global change. Studies on Δ_{leaf} of extant relatives of ancient plants under high temperature and pCO_2 conditions *and* varying degrees of water stress are needed to better interpret changes in $\delta^{13}C_{TOC}$ and $\delta^{13}C_{biomarkers}$ during the PETM and other events.

Conclusions. We document global patterns in Δ_{leaf} among woody plants, including: (*i*) a strong positive correlation with MAP ($R^2 = 0.55$), (*ii*) Δ_{leaf} values 1% to 2.7% lower for EGs than other woody PFTs, and (*iii*) differences up to 6% in Δ_{leaf} among biomes ($R^2 = 0.66$). The relationship of Δ_{leaf} with MAP shows that the balance of leaf gas-exchange in modern plants is largely driven by water availability, consistent with the role of water in driving global trends in ecosystem-scale primary productivity. By revealing global-scale relationships of MAP, PFT, and biome with Δ_{leaf}, our results uniquely enable applications of these patterns for understanding global-scale processes, such as extrapolation of the distribution of PFTs and leaf carbon and water fluxes under future climate scenarios. In geologic studies, our models of Δ_{leaf} provide tools for interpreting spatial and temporal variation in $\delta^{13}C_{TOC}$ and $\delta^{13}C_{biomarkers}$, leading to enhanced understanding of paleoecology and atmospheric CO_2 during climate events that serve as analogs of the near future. Our results warn against the assumption in some geologic studies that Δ_{leaf} is invariant in space and time and emphasize that estimating $\delta^{13}C_{atm}$ from $\delta^{13}C_{TOC}$ or $\delta^{13}C_{leaf}$ requires information about biome, PFT, and paleoclimate. We use this approach to produce a refined estimate of the atmospheric CIE (−4.6%) during the PETM and suggest that it be extended to other PETM CIE records to better estimate T sensitivity to greenhouse gases. Such work will aid our understanding of plant response to extreme climate change both in the geologic past and in the coming century.

Methods

We extracted $\delta^{13}C_{leaf}$ values for woody trees and shrubs from 45 publications and one new study (*SI Appendix*). We excluded $\delta^{13}C_{leaf}$ values from juvenile, fertilized, or watered plants, immature or shaded leaves, and understory shrubs. All $\delta^{13}C_{leaf}$ values were converted to $\Delta^{13}C_{leaf}$ using the Farquhar et al. (10) equation ($\Delta_{leaf} = (\delta^{13}C_{atm} - \delta^{13}C_{leaf})/(1 + \delta^{13}C_{leaf}/10^3)$) and $\delta^{13}C_{atm}$ values estimated for the year of sampling (39) unless reported. Estimating $\delta^{13}C_{atm}$ may cause bias in Δ_{leaf} due to seasonal and latitudinal gradients in $\delta^{13}C_{atm}$. However, this gradient is <0.5% during the growing season (40). Species means were calculated for each geographic site to remove within-species variability. For a subset of sites where $\delta^{13}C_{leaf}$ values from multiple PFTs were reported ($n = 53$), we calculated paired PFT differences at each site by averaging all species in each PFT and then calculating differences between PFT. For each geographic site, environmental factors were extracted from the publication or derived from global databases (*SI Appendix*) and biome classifications were assigned based on the BIOME4 model, descriptions in the original publication, and environmental factors. We analyzed the data using linear, least squares regression and ANOVA (SAS JMP 7.0). Δ_{leaf} values and latitude are approximately normally distributed. MAP was $\log_{10}$-normally distributed and transformed accordingly. Altitude was approximately normally distributed after square root transformation. We performed pairwise comparisons of means using the Tukey-Kramer HSD. Statistics reported within the text and appendices were performed at the site-species combination level, unless otherwise noted ($n = 570$ or less, depending on the model). Similar results were obtained from statistical models at the site level (*SI Appendix*) using means for all species at a site ($n = 73$ or less).

ACKNOWLEDGMENTS. We thank the editors and reviewers for helpful comments. We thank Josh Dorin, Heather Graham, and Clayton Magill for data collection assistance. We also thank David Williams for providing data. This research was supported by the National Science Foundation Grant EAR-0844212 (to K.H.F.), fellowship awards from the Penn State Biogeochemical Research Initiative for Education (BRIE) funded by National Science Foundation Integrative Graduate Education and Research Traineeship (IGERT) Grant DGE-9972759 (to A.F.D. and K.E.M.), and a Department of Energy Graduate Research Environmental Fellowship (GREF) award (to K.E.M.).

1. Bowen GJ, Beerling DJ, Koch PL, Zachos JC, Quattlebaum T (2004) A humid climate state during the Palaeocene/Eocene thermal maximum. *Nature* 432:495–499.
2. Smith FA, Wing SL, Freeman KH (2007) Carbon and hydrogen isotope compositions of plant lipids during the PETM as evidence for the response of terrestrial ecosystems to rapid climate change. *Earth Planet Sci Lett* 262:50–65.
3. Marshall JD, Brooks JR, Lajtha K (2007) Sources of variation in the stable isotopic composition of plants. *Stable isotopes in ecology and environmental science*, eds R Michener and K Lajtha (Wiley-Blackwell, USA), 2nd Ed, pp 22–60.
4. Arens NC, Jahren AH, Amundson R (2000) Can C3 plants faithfully record the carbon isotopic composition of atmospheric carbon dioxide?. *Paleobiology* 26:137–164.
5. Kaplan JO, Prentice C, Buchmann N (2002) The stable carbon isotope composition of the terrestrial biosphere: Modeling at scales from the leaf to the globe. *Global Biogeochem Cycles* 16:1060 doi:10.1029/2001GB001403.
6. Leavitt SW, Newberry T (1992) Systematics of stable-carbon isotopic differences between gymnosperm and angiosperm trees. *Plant Physiol* 11:257–262.
7. Pagani M, Caldeira K, Archer D, Zachos JC (2006) ATMOSPHERE: An ancient carbon mystery. *Science* 314:1556–1557.
8. Hayes JM, Strauss H, Kaufman AJ (1999) The abundance of ^{13}C in marine organic matter and isotopic fractionation in the global biogeochemical cycle of carbon during the past 800 Ma. *Chem Geol* 161:103–125.
9. Wing SL, et al. (2005) Transient floral change and rapid global warming at the Paleocene-Eocene boundary. *Science* 310:993–996.
10. Farquhar GD, Ehleringer JR, Hubick KT (1989) Carbon isotope discrimination and photosynthesis. *Annu Rev Plant Phys* 40:503–537.
11. Seibt U, Rajabi A, Griffiths H, Berry J (2008) Carbon isotopes and water use efficiency: sense and sensitivity. *Oecologia* 155:441–454.
12. Ehleringer JR, Cerling TE (1995) Atmospheric CO_2 and the ratio of intercellular to ambient CO_2 concentrations in plants. *Tree Physiol* 15:105–111.
13. Ehleringer JR, Phillips SL, Comstock JP (1992) Seasonal variation in the carbon isotopic composition of desert plants. *Funct Ecol* 6:396–404.
14. Warren CR, Adams MA (2006) Internal conductance does not scale with photosynthetic capacity: Implications for carbon isotope discrimination and the economics of water and nitrogen use in photosynthesis. *Plant Cell Environ* 29:192–201.
15. Helliker BR, Richter SL (2008) Subtropical to boreal convergence of tree-leaf temperatures. *Nature* 454:511–514.
16. Hemming D, et al. (2005) Pan-european $\delta^{13}C$ values of air and organic matter from forest ecosystems. *Glob Change Biol* 11:1065–1093.
17. Miller JM, Williams RJ, Farquhar GD (2001) Carbon isotope discrimination by a sequence of *Eucalyptus* species along a subcontinental rainfall gradient in Australia. *Funct Ecol* 15:222–232.
18. Schulze E-D, et al. (1998) Carbon and nitrogen isotope discrimination and nitrogen nutrition of trees along a rainfall gradient in northern Australia. *Australian J Plant Physiol* 25:413–425.
19. Swap RJ, Aranibar JN, Dowty PR, Gilhooly WP, III, Macko SA (2004) Natural abundance of ^{13}C and ^{15}N in C3 and C4 vegetation of southern Africa: patterns and implications. *Glob Change Biol* 10:350–358.
20. Warren CR, McGrath JF, Adams MA (2001) Water availability and carbon isotope discrimination in conifers. *Oecologia* 127:476–486.
21. Chapin FS, Matson PA, Mooney HA (2002) *Principles of terrestrial ecosystem ecology* (Springer, New York) p 472.
22. Kelly CK, Woodward FI (1995) Ecological correlates of carbon isotope composition of leaves: A comparative analysis testing for the effects of temperature, CO_2 and O_2 partial pressures and taxonomic relatedness on $\delta^{13}C$. *J Ecol* 83:509–515.
23. Aerts R (1995) The advantages of being evergreen. *Trends Ecol Evol* 10:402–407.
24. Givnish TJ (2002) Adaptive significance of evergreen vs. deciduous leaves: solving the triple paradox. *Silva Fenn* 36:703–743.
25. Schouten S, et al. (2007) The Paleocene-Eocene carbon isotope excursion in higher plant organic matter: Differential fractionation of angiosperms and conifers in the Arctic. *Earth Planet Sci Lett* 258:581–592.
26. Meinzer F (2003) Functional convergence in plant responses to the environment. *Oecologia* 134:1–11.
27. Crisp MD, et al. (2009) Phylogenetic biome conservatism on a global scale. *Nature* 458:754–756.
28. Wilf P (2000) Late Paleocene-early Eocene climate changes in southwestern Wyoming: Paleobotanical analysis. *Geol Soc Am Bull* 112:292–307.
29. Brocks JJ, Summons RE, Heinrich DH, Karl KT (2003) Sedimentary hydrocarbons, biomarkers for early life. *Treatise on Geochemistry* (Pergamon, Oxford), pp 63–115.
30. Bechtel A, Sachsenhofer RF, Zdravkov A, Kostova I, Gratzer R (2005) Influence of floral assemblage, facies and diagenesis on petrography and organic geochemistry of the Eocene Bourgas coal and the Miocene Maritza-East lignite (Bulgaria). *Org Geochem* 36:1498–1522.
31. Peters-Kottig W, Strauss H, Kerp H (2006) The land plant $\delta^{13}C$ record and plant evolution in the Late Palaeozoic. *Palaeogeogr Palaeocl* 240:237–252.
32. Beerling DJ, Royer DL (2002) Fossil plants as indicators of the Phanerozoic global carbon cycle. *Annu Rev Earth Pl Sc* 30:527–556.

33. Wing S, Boucher LD (1998) Ecological aspects of the Cretaceous flowering plant radiation. *Annu Rev Earth Pl Sc* 26:379–421.
34. Jagels R, Day ME (2004) The adaptive physiology of *Metasequoia* to Eocene high-latitude environments. *The evolution of plant physiology*, eds AR Hemsley and I Poole (Linnean Society of London, New York), pp 401–425.
35. McArthur JV, Moorhead KK (1996) Characterization of riparian species and stream detritus using multiple stable isotopes. *Oecologia* 107:232–238.
36. Handley L, Pearson PN, McMillan IK, Pancost RD (2008) Large terrestrial and marine carbon and hydrogen isotope excursions in a new Paleocene/Eocene boundary section from Tanzania. *Earth Planet Sci Lett* 275:17–25.
37. McCarren H, Thomas E, Hasegawa T, Röhl U, Zachos JC (2008) Depth dependency of the Paleocene-Eocene carbon isotope excursion: Paired benthic and terrestrial biomarker records (Ocean Drilling Program Leg 208, Walvis Ridge). *Geochem Geophy Geosyst 9* p Q10008 doi:10.1029/2008GC002116.
38. Jahren AH, Arens NC, Harbeson SA (2008) Prediction of atmospheric $\delta^{13}CO_2$ using fossil plant tissues. *Rev Geophys* 46 RG1002, doi:10.1029/2006RG000219.
39. McCarroll D, Loader NJ (2004) Stable isotopes in tree rings. *Quaternary Science Reviews* 23:771–801.
40. GLOBALVIEW-CO2C13 (2008) Cooperative atmospheric data integration project—$\delta^{13}C$ of carbon dioxide. (NOAA ESRL, Boulder, Colorado) http://www.esrl.noaa.gov/gmd/ccgg/globalview/co2c13/co2c13_intro.html.

Supporting Information Appendix

Diefendorf, Mueller, Wing, Koch and Freeman

Supporting Information Table of Contents

Dataset Description

Our data set, provided in Supporting Information (SI) Dataset, includes 334 species from 75 plant families (limited to woody trees and shrubs) present at 105 geographic sites distributed across 5 continents (representing 3,310 $\delta^{13}C_{leaf}$ measurements of individual plants). The result is 570 unique species-site combinations represented by a mean Δ_{leaf} value calculated from individuals of each species at a site. Sites are located within 8 biomes with mean annual temperature (MAT) ranging from -10 to 28°C and mean annual precipitation (MAP) from 147 to 3700 mm per year. $\delta^{13}C_{leaf}$ values were converted to $\Delta^{13}C_{leaf}$ using the equation $\Delta_{leaf} = (\delta^{13}C_{atm} - \delta^{13}C_{leaf})/(1+\delta^{13}C_{leaf}/10^3)$ with estimated or measured $\delta^{13}C_{atm}$ values (See SI Dataset). Δ_{leaf} values and latitude are approximately normally distributed. MAP and summer precipitation (P-JJA; June, July, August) were Log_{10}-normally distributed and transformed accordingly. Altitude was approximately normally distributed after square root transformation (Sqrt altitude). Species means were calculated for each geographic site to remove within-species variability. For a subset of sites where $\delta^{13}C_{leaf}$ values from multiple PFTs were reported (n=53), we calculated paired PFT differences at each site by averaging all species in each PFT and then calculating differences between PFT.

SI Data Analysis

Table 1) Linear regression of Δ_{leaf} with environmental variables at the global scale.

Environmental Variable	R^2	Slope	*p* value	n
$Log_{10}MAP^*$	0.55	+	<0.0001	506
Sqrt altitude	0.40	-	<0.0001	502
MAT	0.33	+	<0.0001	506

* Log_{10}MAP is highly correlated with sqrt altitude (r = -0.59, *p*<0.0001, n = 501), MAT (r = 0.70, *p*<0.0001, n = 505), latitude (r = -0.78, *p*<0.0001, n = 505), and could be related to other environmental parameters not available in our global dataset. See Table 3, 4, and 5 (below) for multiple regression results.

Table 2) Linear regression of Δ_{leaf} with MAP, P-JJA, and altitude by geographic zone.

	Log_{10}MAP			Log_{10}P-JJA*			Sqrt altitude		
Geographic zone	R^2	*p* value	n	R^2	*p* value	n	R^2	*p* value	n
Global†	0.548	<0.0001	506	0.24	<0.0001	194	0.403	<0.0001	502
Global (excluding Europe)	0.579	<0.0001	411	0.316	<0.0001	130	0.443	<0.0001	407
Asia	0.486	<0.0001	62	0.23	0.029	21	0.089	0.023	58
Europe	0.025	0.125	95	0.008	0.486	64	0.056	0.021	95
North America	0.42	<0.0001	177	0.332	<0.0001	109	0.452	<0.0001	171

Other continents in our database were excluded from these analyses due to small numbers of geographic sites (e.g. South America). *Summer precipitation in tropical sites was not included because precipitation is more evenly distributed during the year. †The global Δ_{leaf} relationship with MAP (mm/yr) is as follows (standard error shown in parentheses):

$$\Delta_{leaf} = 5.54(\pm 0.22) * \log_{10}(MAP) + 4.07(\pm 0.70)$$

Table 3) Multiple regression of Δ_{leaf} with MAP and altitude by geographic zone.

Geographic zone	R^2	*p* value	n	Log_{10}MAP SS* (partial R^2)	Sqrt altitude SS* (partial R^2)
Global†	0.607	<0.0001	502	646.2 (0.34)	187.9 (0.13)
Global (excluding Europe)	0.622	<0.0001	407	483.2 (0.32)	117.9 (0.10)
Asia	0.507	<0.0001	58	136.2 (0.46)	16.3 (0.09)
Europe	0.122	0.003	95	15.4 (0.07)	22.7 (0.10)
North America	0.534	<0.0001	177	78.6 (0.15)	108.8 (0.20)

Other continents in our database were excluded from these analyses due to small numbers of geographic sites (e.g. South America). *SS is the sum of squares. SS and partial R^2 values are listed only for parameters with significant effects in the model (alpha=0.05). †The global Δ_{leaf} relationship with MAP (mm/yr) and altitude (m) is as follows (standard error shown in parentheses):

$$\Delta_{leaf} = 4.20(\pm 0.26) * \log_{10}(MAP) - 0.06(\pm 0.01) * \sqrt{altitude} + 9.31(\pm 0.90)$$

We constrained multiple regression models of Δ_{leaf} variability to include both MAP and altitude, which were the strongest predictors of Δ_{leaf} variability in single factor regression models (excluding other measures of water availability that are highly correlated with MAP, but less well correlated with Δ_{leaf}). The inclusion of MAP in all models is also justified because the influence of MAP on Δ_{leaf} is well supported by theory and other observations. Since MAP is correlated with other potential predictor variables (Table 1 caption), care is required in evaluating these predictors for their additional influence on Δ_{leaf}. Therefore, we first assessed the influence of other factors on Δ_{leaf} using bivariate partial regression models that account for the covariance of MAP with secondary predictors (e.g. by plotting the residuals of Δ_{leaf} from its regression with MAP versus the residuals of altitude from its regression with MAP). The partial regression model with altitude as the secondary predictor was the only model with notable explanatory power (R^2=0.13, p<0.0001), indicating that altitude has a weak, negative influence on Δ_{leaf} that is statistically independent from MAP. In this manner altitude was determined to be the predictor with the second greatest explanatory power at the global scale. The regression models reported in Table 3 were then constrained to contain MAP and altitude for the purposes of evaluating the consistency of results within different geographic regions. Although these methods cannot determine how much of the variance explained by the regression between MAP and Δ_{leaf} is due to the covariance of MAP and altitude, they consistently show that altitude has an influence on MAP that cannot be explained by its correlation with MAP alone (see also Table 4 below).

The use of forward, backward, or mixed stepwise regression with additional predictors produces models with greater R^2 (up to 0.66 compared to 0.61 for the two factor model at the global scale) and with additional statistically significant predictors. However, the large number of factors required to achieve this minor R^2 improvement drastically reduces the utility and interpretability of the model. For global-scale analyses, three factor models (constrained to contain MAP and altitude, plus a third variable) do not yield an R^2 greater than 0.61, nor do they produce a third factor of statistical significance (p<0.05).

Table 4) Multiple regression of Δ_{leaf} with MAP and altitude for each plant functional type and well-represented genera.

PFT* or G*enera*†	R^2	*p* value	n	Log_{10}MAP SS (partial R^2) ‡	Sqrt altitude SS (partial R^2) ‡
EA	0.612	<0.0001	213	277.7 (0.39)	15.6 (0.03)
DG	0.281	0.037	23	ns	5.3
DA	0.327	<0.0001	175	50.8 (0.12)	33 (0.08)
EG	0.534	<0.0001	82	98.2 (0.37)	56.4 (0.25)
Acer	0.814	<0.001	12	6.9 (0.43)	20.7 (0.70)
Larix	0.307	0.031	22	2 (0.14) ms	5.7 (0.31)
Picea	0.094	ns	25	ns	ns
Pinus	0.702	<0.0001	36	64.2 (0.52)	32.8 (0.36)
Quercus	0.411	<0.001	32	4.6 (0.12) ms	5.7 (0.15)

*Plant functional types are as follows: Deciduous angiosperm (DA), deciduous gymnosperm (DG), evergreen angiosperm (EA), and evergreen gymnosperm (EG). †Only genera with at least 10 species-site combinations are included. ‡SS is the sum of squares. SS and partial R^2 values are listed only for parameters with significant effects in the model (α=0.05). ns = not significant, ms = marginally significant (p<0.1). §The within PFT Δ_{leaf} relationship with MAP (mm/yr) and with MAP and altitude (m) are presented below (standard error shown in parentheses). Please see discussion in SI PETM (below) for application of these models.

EA:

$$\Delta_{leaf} = 5.37(\pm 0.30) * \log_{10}(MAP) + 5.06(\pm 1.00)$$

$$\Delta_{leaf} = 4.64(\pm 0.40) * \log_{10}(MAP) - 0.04(\pm 0.01) * \sqrt{altitude} + 7.99(\pm 1.45)$$

DG: Based on the lack of significance of the regression model (see above), we do not report an equation for DG.

DA:

$$\Delta_{leaf} = 3.14(\pm 0.39) * \log_{10}(MAP) + 11.58(\pm 1.23)$$

$$\Delta_{leaf} = 2.18(\pm 0.45) * \log_{10}(MAP) - 0.04(\pm 0.01) * \sqrt{altitude} + 15.23(\pm 1.51)$$

EG:

$$\Delta_{leaf} = 5.38(\pm 0.76) * \log_{10}(MAP) + 3.16(\pm 2.18)$$

$$\Delta_{leaf} = 4.67(\pm 0.68) * \log_{10}(MAP) - 0.06(\pm 0.01) * \sqrt{altitude} + 7.07(\pm 2.05)$$

Table 5) Multiple regression of Δ_{leaf} with MAP, altitude and latitude or MAT for select plant functional types.

PFT*	R^2	*p* value	n	Log_{10}MAP SS† (partial R^2)	Sqrt altitude SS† (partial R^2)	Latitude SS† (partial R^2)	MAT SS† (partial R^2)
DA	0.378	<0.0001	175	77.4 (0.18)	37.5 (0.10)	28.5 (0.08)	na
DA	0.39	<0.0001	175	85.4 (0.20)	62.9 (0.15)	na	35.5 (0.09)
EG	0.572	<0.0001	82	109.5 (0.42)	30.4 (0.17)	13.6 (0.08)	na
EG	0.547	<0.0001	82	100.3	57.2	na	ns

*See Table 4 for PFT abbreviations. na = not applicable, ns = not significant. SS and partial R^2 values are listed only for parameters with significant effects in the model (α=0.05).

Table 6) Mean Δ_{leaf} and Δ_{leaf} residual values (corrected for MAP and altitude) for each plant functional type.

PFT*	Δ_{leaf}	Level†	n	Δ_{leaf} residuals‡	Level†	n
EA	22.6	A	225	0.4	A	213
DG	20.5	B	26	0.4	AB	23
DA	21.1	B	198	-0.1	B	175
EG	18.4	C	112	-1.1	C	82

*See Table 4 for PFT abbreviations. †Tukey-Kramer HSD levels comparison of mean Δ_{leaf} and mean residual Δ_{leaf} for each PFT; PFTs not connected by same letter are significantly different (p<0.05). ‡Δ_{leaf} residuals are the residuals of Δ_{leaf} after multiple regression with MAP and altitude.

Table 7) 'Paired-site' Δ_{leaf} PFT differences.*

Paired PFT†	Δ_{leaf} difference	Level‡	n
DA-EG	2.7	A	17
EA-EG	2.2	AB	12
DG-EG	1.5	B	21
DA-EA	0.2	C	16

*Paired-sites are sites that contain more than one PFT. Differences between PFTs at each site were calculated and then the mean difference was determined for all sites containing the relevant PFT pair. †See Table 4 for PFT abbreviations. ‡Tukey-Kramer HSD levels comparison of paired-PFTs mean Δ_{leaf} differences; paired-PFT differences not connected by same letter are significantly different (p<0.05) from each other.

Table 8) Mean Δ_{leaf} values for plant functional types within each geographic zone.

	DA*			DG			EA			EG		
Geographic zone	Δ_{leaf} mean	n	Level†	Δ_{leaf} mean	n	Level	Δ_{leaf} mean	n	Level	Δ_{leaf} mean	n	Level
Global	21.1	198	B	20.5	26	B	22.5	225	A	18.4	112	C
Asia	20.4	6	B	20.2	4	B	23.5	40	A	19.6	12	B
Europe	20.4	49	A	20.7	11	A	19.9	27	AB	19.3	44	B
N. America	20.8	91	A	20.4	11	A	20.5	41	A	17.5	56	B

*See Table 4 for PFT abbreviations. †Tukey-Kramer HSD levels comparison of mean Δ_{leaf} values for each PFT, by geographic zone. Geographic zones not connected by same letter are significantly different (p<0.05) from other biomes.

Table 9) Mean Δ_{leaf} values by biome type.

Biome*	Δ_{leaf}	Level†§	n	Level† (with CCF)	n (with CCF)
TRF	23.4	A	206	A	206
EWMF	22.2	B	29	B	29
TSF	21.5	BC	47	B	47
CCDF	21.1	BCD	5	na	na
MED	20.6	CDE	5	BC	5
CCF‡	19.8	na	na	C	136
CCEF	19.9	DE	53	na	na
TDF	19.6	E	26	C	26
CCMF	19.6	E	78	na	na
XWS	17.3	F	59	D	59

*Biomes are as follows: tropical rain forest (TRF), evergreen warm mixed forest (EWMF), tropical seasonal forest (TSF), cool cold deciduous forest (CCDF), mediterranean (MED), cool cold evergreen forest (CCEF), cool cold mixed forest (CCMF), cool cold forest (CCF), tropical deciduous forests (TDF), and xeric woodland/scrubland (XWS) †Tukey-Kramer HSD levels comparison of mean Δ_{leaf} values for each biome. Biomes not connected by same letter are significantly different (p<0.05) from other biomes. ‡CCF is a combined biome including CCDF, CCEF, and CCMF and is not included in the Tukey-Kramer HSD tests. §Biome accounts for 66% of the variability in Δ_{leaf} values (based on R^2 value from ANOVA; p<0.0001, n=508). na = not applicable.

Table 10) Mean Δ_{leaf} values for plant functional types within each biome.

	DA†			DG			EA			EG		
Biome*	Δ_{leaf}	n	Level‡	Δ_{leaf}	n	Level	Δ_{leaf}	n	Level	Δ_{leaf}	n	Level
CCF	20.5	43	A	20.3	24	A	19.5	14	AB	19.1	55	B
EWMF	22.5	19	A	20.9	1	A	21.9	4	A	21.3	5	A
TDF	20.0	19	A	na	na	na	18.7	7	B	na	na	na
MED	22.6	1	na	na	na	na	20.1	4	na	na	na	na
TRF	22.5	51	A	na	na	na	23.8	144	B	20.1	2	A
TSF	21.6	22	A	na	na	na	22.1	16	A	na	na	na
XWS	18.6	14	A	na	na	na	18.6	17	A	15.9	28	B

*See Table 9 for biome abbreviations. †See Table 5 for PFT abbreviations. ‡Tukey-Kramer HSD levels comparison of PFT mean Δ_{leaf} values within each biome; PFTs not connected by the same letter are significantly different (p<0.05). na = not applicable.

Table 11) Linear regression of "site-mean*" Δ_{leaf} values with environmental variables at the global scale.

Environmental Variable	R^2	Slope	p value	n
Log_{10}MAP	0.52	+	<0.0001	70
Sqrt altitude	0.40	-	<0.0001	69
MAT	0.17	+	=0.0004	70

*Site-means are calculated by averaging all Δ_{leaf} values at a site, regardless of PFT. Sites with single species present are not included to avoid biasing the results by single species values.

Table 12) Multiple regression of "site-mean[*]" Δ_{leaf} values by MAP and altitude by geographic zone.

Geographic zone	R^2	*p* value	n	Log_{10}MAP SS[†]	Sqrt altitude SS[†]
Global	0.725	<0.0001	69	76.9 (0.54)	49.0 (0.43)
Asia	0.833	0.0047	9	21.9 (0.83)	3.0 (0.39)
Europe	0.200	0.1	23	4.6 (0.15) ms	4.7 (0.16) ms
North America	0.749	<0.0001	32	12.8 (0.48)	30.8 (0.64)

[*]Site-means are calculated by averaging all Δ_{leaf} values at a site, regardless of PFT. Sites with single species present are not included to avoid biasing the results by single species values. [†]SS is the sum of squares. SS and partial R^2 values are listed only for parameters with significant effects in the model (alpha=0.05). ms = marginally significant ($p<0.1$). Multiple regression analyses were performed as described in the caption of Table 3 (above).

Table 13) ANOVA of "site-mean[*]" Δ_{leaf} values by biome.

Biome[†‡]	Δ_{leaf} mean	n	Level[#]
TRF	23.4	6	A
EWMF	21.8	6	AB
TSF	21.0	3	BC
MED	20.6	1	
CCF[§]	19.7	39	C
TDF	19.4	2	CD
XWS	17.4	15	D

[*]Site-means are calculated by averaging all Δ_{leaf} values at a given site, regardless of PFTs present. [†] See Table 9 for biome abbreviations. [‡]Biome accounts for 76% of the variability in site-mean Δ_{leaf} values (based on R^2 from ANOVA; $p<0.0001$, n=69). MED is excluded from ANOVA because the sample size is too small (n=1). [§]CCF includes CCDF, CCMF, and CCEF. [#]Tukey-Kramer HSD levels comparison of biomes within each PFT; Biomes not connected by the same letter are significantly different ($p<0.05$).

SI Figures

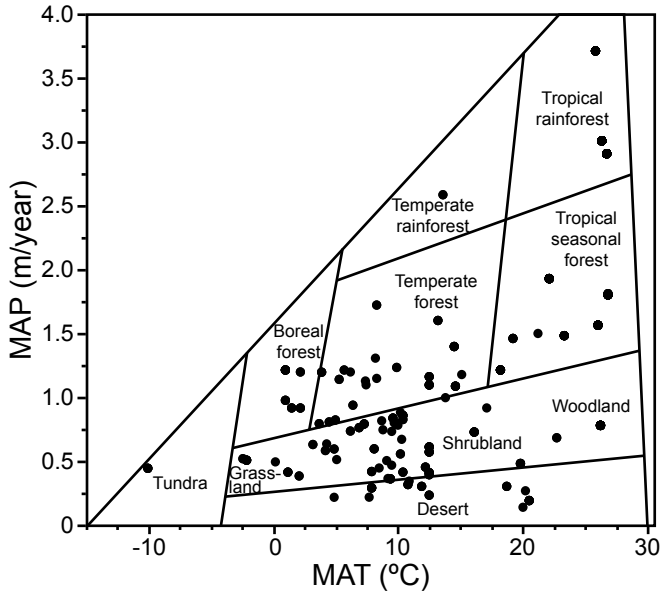

SI Figure 1. Mean annual temperature (MAT) and mean annual precipitation (MAP) for sites reported in text and S1 where environmental information was available. Biome types of Whitaker (1) are given for general reference and differ from the biome classification used within the text and data analysis (see methods section).

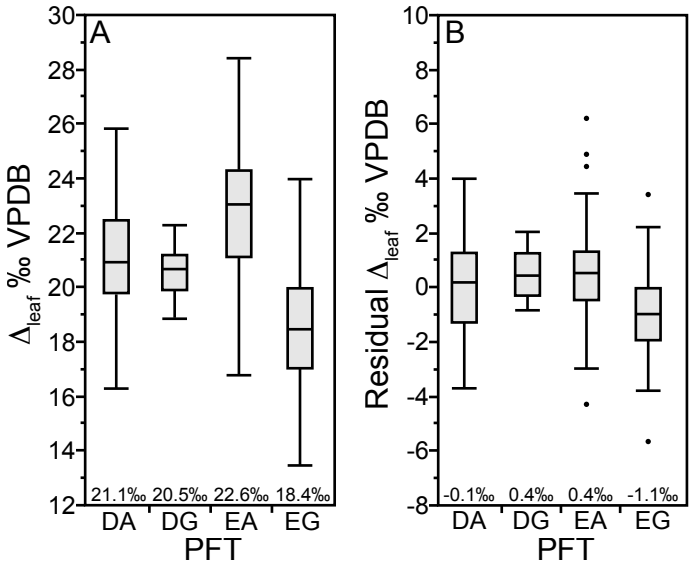

SI Figure 2. Box plots of A) Δ_{leaf} values by PFT (n: DA=198, DG=26, EA=225, EG=112) and B) Δ_{leaf} residuals (after constraining for MAP and altitude) by PFT (n: DA=175, DG=23, EA=213, EG=82). The box contains the interquartile range (50% of the central population). The median sample value is denoted by the line within the box. Vertical lines extend outward to the minimum and maximum values, except in the case of samples that fall outside 1.5 times the interquartile range (denoted with black dots). Statistical tests of means are sown in SI Data Analysis (above).

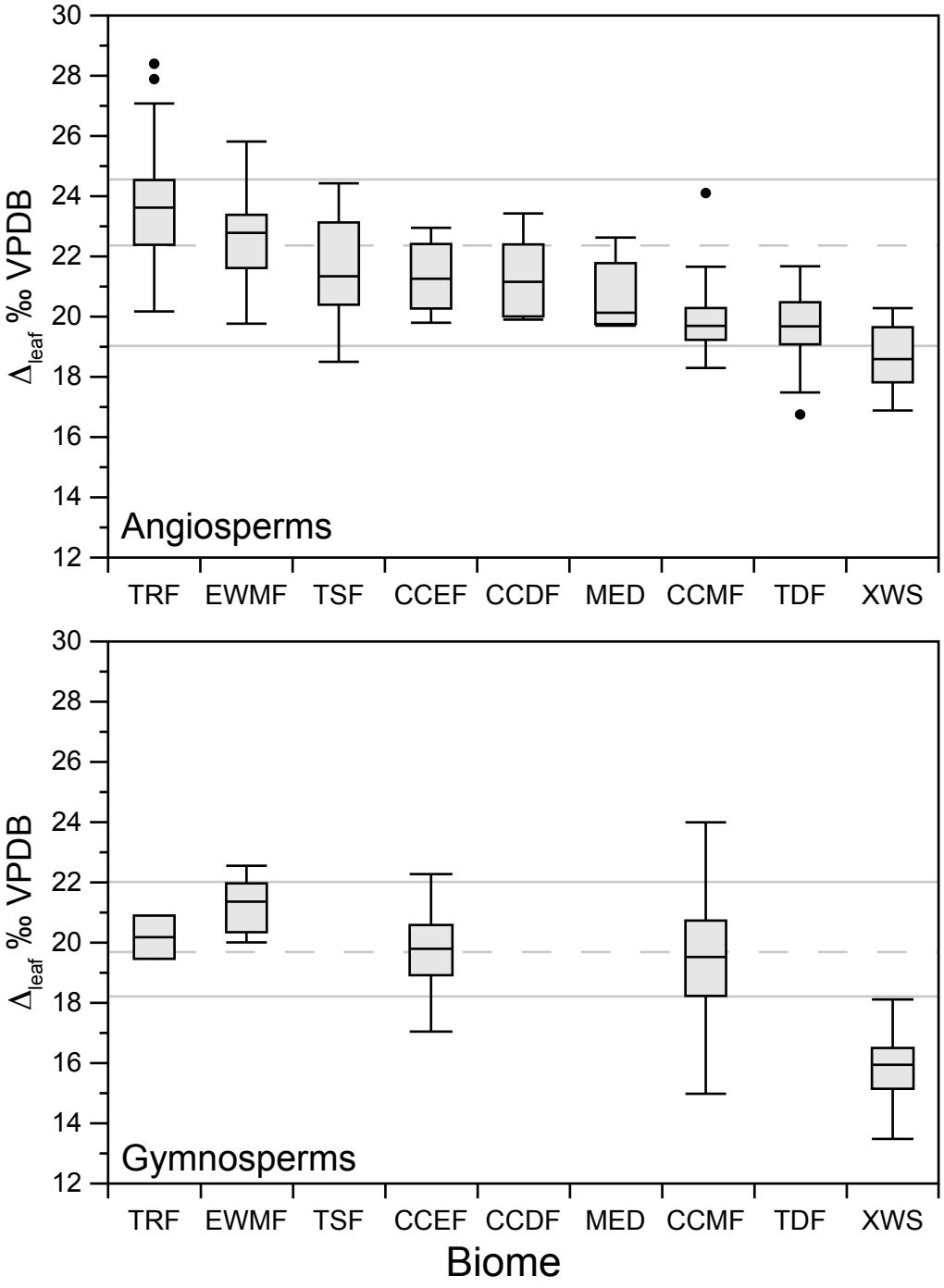

SI Figure 3. Biome-level Δ_{leaf} differences as a function of phylogeny. Biome-level box plots of Δ_{leaf} values separated by phylogeny. The box contains the interquartile range (50% of the central population). The median sample value is denoted by the line within the box. Vertical lines extend outward to the minimum and maximum values, except in the case of samples that fall outside 1.5 times the interquartile range (denoted with black dots). Dashed horizontal lines denote the grand means of the populations (excluding XWS; angiosperm=22.3‰ and gymnosperm=19.7‰). The 2.6‰ difference between these grand Δ_{leaf} means reflects the PFT differences reported in the discussion section. Solid horizontal lines are shown to emphasize the Δ_{leaf} ranges observed in biomes between the phylogenies (excluding XWS). Number of samples per biome for angiosperms is as follows: CCDF=5, CCEF=8, CCMF=44, EWMF=23, MED=5, TDF=26, TRF=204, TSF=47, and XWS=31. For the gymnosperms: CCEF=45, CCMF=34, EWMF=6, TRF=2, and XWS=28.

SI PETM Discussion

Calculation of PETM Δ_{leaf} Values: The conceptual diagram of $\delta^{13}C_{atm}$ reconstruction for the Paleocene-Eocene Thermal Maximum (PETM) in Bighorn Basin (WY, USA) was determined from $\delta^{13}C_{leaf}$ values as inferred from $\delta^{13}C$ values of *n*-C_{31} alkanes (corrected for biosynthetic fractionation; (2)). The percent angiosperm and MAP values were derived from fossil leaf metrics (3, 4) and we make the assumption that *n*-alkane production in plants is similar across PFTs. We used Δ_{leaf}-MAP expressions for deciduous angiosperms (DA) and evergreen gymnosperms (EG; see SI Data Analysis Table 4 for determination of expressions):

$$\Delta_{leaf}(\mathrm{DA}) = 3.14(\pm 0.39) * \log_{10}(MAP) + 11.58(\pm 1.23)$$

$$\Delta_{leaf}(\mathrm{EG}) = 5.38(\pm 0.76) * \log_{10}(MAP) + 3.16(\pm 2.18)$$

To determine a net Δ_{leaf} value, we scaled the Δ_{leaf} values by the percentage of angiosperm and, by difference, conifer. $\delta^{13}C_{atm}$ was then calculated:

$$\delta^{13}C_{atm} = \Delta_{leaf} * \left[1 + \frac{\delta^{13}C_{leaf}}{1000}\right] + \delta^{13}C_{leaf}$$

This results in minor changes to net Δ_{leaf} during the PETM (Fig. 4) because the MAP and PFT influences nearly cancel each other out. We note that this is likely not the case in other studies. For example, if MAP increases and there is a shift from conifers to angiosperms, Δ_{leaf} could change by several ‰ resulting in much larger corrections on $\delta^{13}C_{leaf}$ than in our example.

Table of Δ_{leaf} and $\delta^{13}C_{atm}$ estimates for the PETM in the Bighorn Basin (WY, USA).

Age*	Meters*	$\delta^{13}C_{leaf}$*	% Angio.*	MAP (mm/yr)†	Δ_{leaf} (DA)‡	Δ_{leaf} (EG)‡	Net Δ_{leaf}‡	$\delta^{13}C_{atm}$‡
54.30	73.30	-27.1	23	1380	21.4	20.1	20.4	-7.3
54.80	45.30	-27.2	23	1380	21.4	20.1	20.4	-7.4
55.00	37.30	-29.7	23	1440	21.5	20.2	20.5	-9.9
55.65	8.20	-31.6	99	800	20.7	18.8	20.6	-11.6
55.75	-0.15	-31.1	99	800	20.7	18.8	20.6	-11.1
55.80	-0.85	-31.7	99	800	20.7	18.8	20.6	-11.7
56.00	-13.75	-26.6	23	1380	21.4	20.1	20.4	-6.8
56.20	-19.75	-26.8	23	1380	21.4	20.1	20.4	-7.0

*Age (Ma), section meters, $\delta^{13}C_{leaf}$ (‰ VPDB), and % Angiosperm (Angio) are from Smith et al. (2). †MAP is from Wing et al. (3) and Wilf (4). ‡Calculations are described above.

Suggested use of Δ_{leaf} models: We use Δ_{leaf} expressions calculated separately for each PFT as opposed to using the global Δ_{leaf} expression because the slope of the relationship between Δ_{leaf} and MAP differs according to PFT, and this allows us to account for MAP and PFT controls on Δ_{leaf} simultaneously. We caution that the magnitude of MAP and PFT corrections applied to terrestrial isotope records using this approach is sensitive to the slope and intercept estimated in our statistical models. Future additions to our global dataset will provide additional refinement of our models and enable further evaluation of our corrections to Δ_{leaf} and $\delta^{13}C_{atm}$. An assumption of this approach is that MAP is a reasonable estimate of water availability for the plants from which TOC or biomarker isotope records are derived.

SI Methods

Climate data. Mean annual precipitation (MAP) and mean summer (June, July, and August) precipitation (P-JJA) were derived from multiple sources due to differences in the quality of data available across sites. Summer precipitation was estimated using June, July and August only for sites in temperate or arctic latitudes. We did not have sites in these seasonal latitudes from the Southern hemisphere. Precipitation data were derived from the following three sources, listed in order of priority with respect to inclusion: 1) the 1971-2000 PRISM 800 meter resolution model (PRISM Group, Oregon State University, http://www.prismclimate.org, created Feb 17 2009), 2) values reported in the publication, or 3) the 1951-2000 0.5º x 0.5º GPCC normals data set (Global Precipitation Climate Center; http://gpcc.dwd.de). The PRISM model contained the highest geographic specificity, however is only available for the United States of America; it is highly correlated with GCCP values (R^2=0.80, p<0.0001) despite differences in resolution. Mean annual temperature (MAT) and mean summer temperature (T-JJA) were derived from the 1991-2000 0.5 X 0.5º CRU TS 2.1 data set (5). Additional climate parameters were also compiled from FAO gridded data sets (e.g., available soil moisture, vapor pressure, sunlight percentage, a continentality index, etc. see SI Dataset).

References

1. Whittaker R (1975) *Communities and Ecosystems, 2nd edn* (MacMillan, New York) p 167.
2. Smith FA, Wing SL, Freeman KH (2007) Carbon and hydrogen isotope compositions of plant lipids during the PETM as evidence for the response of terrestrial ecosystems to rapid climate change. *Earth Planet Sci Lett* 262:50-65.
3. Wing SL*, et al.* (2005) Transient Floral Change and Rapid Global Warming at the Paleocene-Eocene Boundary. *Science* 310:993-996.
4. Wilf P (2000) Late Paleocene-early Eocene climate changes in southwestern Wyoming: Paleobotanical analysis. *Geo Soc Am Bull* 112:292-307.
5. Mitchell TD, Jones PD (2005) An improved method of constructing a database of monthly climate observations and associated high-resolution grids. *Int J Clim* 25:693-712.